



Article

Shrinkage of Micro-Synthetic Fiber-Reinforced Mortar

Endah Safitri, Ridan Adi Kusworo and Stefanus Adi Kristiawan *

SMARTCrete Research Group, Civil Engineering Department, Sebelas Maret University, Kota Surakarta 57126, Indonesia

* Correspondence: s.a.kristiawan@ft.uns.ac.id

Abstract: Repair materials have been developed in this research by adding micro-synthetic fibers in cement-based mortar. In addition, accelerator is incorporated in the mortar to obtain high early strength of the repair materials. Their shrinkage behavior is of interest. This study aims to determine the shrinkage of the micro-synthetic fiber-reinforced mortar and propose models to reflect their shrinkage behavior. The results show that rapid developments of shrinkage are observed at an early age where the 3-day shrinkage already attains about 40–50% of the 84-day shrinkage value. Moreover, after 14 days of age the shrinkage curves tend to approach the asymptotic value. The ACI 209.2R-08 and CEB-MC 90-99 models do not reflect the shape of the shrinkage curves of the micro-synthetic fiber-reinforced mortar. Therefore, this research proposes a modified ACI 209.2R-08 and CEB-MC 90-99 that can describe the shrinkage behavior of the micro-synthetic fiber-reinforced mortar. The accuracy of the modified models has been confirmed quantitatively using the method of best fit line, residual analysis, and coefficient of error.

Keywords: micro fiber; shrinkage; shrinkage prediction model; repair mortar



Citation: Safitri, E.; Kusworo, R.A.; Kristiawan, S.A. Shrinkage of Micro-Synthetic Fiber-Reinforced Mortar. *Infrastructures* **2023**, *8*, 7. <https://doi.org/10.3390/infrastructures8010007>

Academic Editor: Pedro Arias-Sánchez

Received: 19 October 2022

Revised: 18 December 2022

Accepted: 28 December 2022

Published: 31 December 2022



Copyright: © 2022 by the authors. Licensee MDPI, Basel, Switzerland. This article is an open access article distributed under the terms and conditions of the Creative Commons Attribution (CC BY) license (<https://creativecommons.org/licenses/by/4.0/>).

1. Introduction

Damage of concrete to various extents may be observed in structural concrete building and it affects the strength and serviceability of the structure. Therefore, repair to the particular damage is necessary to restore the safety and functionality of the concrete structure [1–3]. Moreover, good repair to the damaged concrete can improve the overall performance of concrete structures, increase their strength and stiffness, improve the appearance of concrete surfaces, make them watertight, and prevent aggressive substances from entering the steel surface [4]. A variety of repair systems are available today, and their pertinence is governed by the type of damage. For example, the patch repair system is a method suitable for recovering the spalling of concrete [5,6].

One repair material for concrete patching is cement-based mortar. However, cement-based mortar is known to have relatively low tensile strength when compared to its compressive strength. As a result, the repair material will be at a high risk of cracking due to the emergence of tensile stress induced by the differential shrinkage between the repair material and the concrete substrate [7,8]. Therefore, randomly dispersed micro-fibers can be incorporated into the mixture of this cement-based mortar to increase its tensile strength and toughness properties [9,10]. The increase in these properties is governed by the capability of the micro-fibers to prevent or control the initiation, propagation, or coalescence of cracks [11], so that the mortar with added micro-fiber material can improve its resistance against cracking due to the differential shrinkage stress that occurred in the patching system [12,13].

Shrinkage in concrete can be related to the loss of water content in the capillary pores due to drying. Several studies showed a linear relationship between drying shrinkage and water loss [14,15]. Shrinkage must be carefully assessed as it affects the durability of repair material as indicated in the preceding paragraph. When two materials with different shrinkage properties are combined, such as in repairing a concrete structure with repair

material, it creates a restraint. In this case, the higher shrinkage of repair material will be restrained by the concrete layer that has a lower shrinkage. As a result of this restraint, a tensile strain is induced in the repair layer and may cause the repair material to crack, if this tensile strain reaches the maximum tensile capacity of the repair material [16].

Shrinkage originates from the cement paste, while the aggregate is considered an inert material. Nevertheless, it has been shown that the composition of the mixture contained in the mortar/concrete affects the magnitude of shrinkage. For example, it was found that the addition of polypropylene fiber at 0.1% and 0.2% content could reduce the shrinkage of high-performance concrete [17]. It is also shown that the addition of a non-alkaline accelerator can increase shrinkage during the initial drying period [18].

The purpose of this study is to determine the effect of adding synthetic microfibers to repair mortar on shrinkage behavior. Moreover, this research also aims to propose modified shrinkage prediction models to estimate the shrinkage behavior of micro-synthetic fiber-reinforced mortar. The results will be valuable, especially to assess the risk of shrinkage cracking of micro-synthetic fiber-reinforced mortar when it is used as a repair material.

2. Shrinkage Prediction Models

Shrinkage of concrete tends to increase with time at a decelerating rate. Subsequently, a model for predicting shrinkage as a function of time forms a hyperbolic curve with an asymptotic value. The asymptotic value represents the ultimate shrinkage. Such a model can be expressed in terms of the ultimate shrinkage value multiplied by the time ratio to describe the shrinkage development with time. An example of the model is given in ACI 209.2R-08 [19]. In the same document, alternative models for predicting shrinkage with time are also mentioned, one of which is CEB-MC 90-99 [20]. The shape of the shrinkage curve estimated by the models depends on many factors, including mixture proportioning. Thus, it might be necessary to modify the models to accurately depict the shape of the shrinkage curve for a particular concrete type [21–23].

The following shrinkage prediction models will be applied to estimate the shape of the shrinkage curve of the micro-synthetic fiber-reinforced mortar investigated in this study:

(a) ACI 209.2R-08

The general model for predicting shrinkage strain, $\epsilon_{sh}(t, t_c)$, at concrete age, t (days), measured after the start of drying at t_c is given by Equation (1).

$$\epsilon_{sh}(t, t_c) = \left(\frac{t - t_c}{f + t_c} \right) \times \epsilon_{sh(u)} \tag{1}$$

where $\epsilon_{sh(u)}$ is the ultimate shrinkage value, t_c is the start of concrete drying which equals the end of the curing time, and f is the shrinkage half-time in days, i.e., the time representing the shrinkage reaching half of the ultimate value. The shrinkage half-time signifies the shape of the curve and its value depends on the curing of concrete. ACI 209.2R-08 recommends 35 and 55 for 7 days of moist curing and 1–3 days of steam curing, respectively. The higher value of f implies a lower rate of shrinkage development at an early time. Subsequently, for shrinkage of particular concrete which shows a different rate of shrinkage development at an early age than normal concrete, a different value of f may be suggested to accurately represent such behavior.

(b) CEB-MC 90-99

The shrinkage prediction model by CEB-MC 90-99 is presented in the following equations:

$$\epsilon_{sh}(t, t_c) = \epsilon_{cso} \beta_s(t - t_c) \tag{2}$$

$$\beta_s(t - t_c) = \left[\frac{(t - t_c)/t_1}{350[(V/S)/(V/S_0)]^2 + (t - t_c)/t_1} \right]^{0.5} \tag{3}$$

where $\varepsilon_{sh(t,t_c)}$ is the shrinkage of concrete at age of t measured after time of curing t_c , ε_{cs0} is the notional shrinkage coefficient representing the asymptotic behavior of the curve shape, $\beta_s(t - t_c)$ is the coefficient describing the shrinkage development with a time of drying $(t - t_c)$, t_1 is equal to 1 day, (V/S) is volume to surface ratio, (V/S_0) is equal to 50 mm. The constant value of 350 in Equation (3) signifies the rate of shrinkage development at an early age and, thus, affects the shape of the shrinkage curve at an early age in a similar manner to the shrinkage half-time of the ACI 209.2R-08 model.

The accuracy of the two models may be evaluated by the method of best fit line, residual values (R), or the coefficient of error values (M) [22]. The best fit line is a method derived from a linear regression analysis of the laboratory shrinkage data versus the predicted value. The residual values (R) method is determined from the difference between the predicted shrinkage minus the laboratory shrinkage data. A positive value of R indicates that the predicted shrinkage exceeds the test data, and vice versa. The coefficient of error M is calculated by Equation (4) as follows:

$$M = \frac{1}{\overline{\varepsilon_{sh(t)}}} \sum \left\{ \frac{(\varepsilon_{sh(t)} - \varepsilon'_{sh(t)})^2}{n} \right\}^{1/2} \times 100\% \quad (4)$$

where $\varepsilon_{sh(t)}$ is the laboratory shrinkage value at time t , $\varepsilon'_{sh(t)}$ is the predicted shrinkage value at time t , $\overline{\varepsilon_{sh(t)}}$ is the average of the laboratory shrinkage values, and n is the number of shrinkage data.

The ACI 209.2R-08 and CEB-MC 90-99 models may be modified to represent the shrinkage behavior of a particular concrete type. The modified models should give a shape of the curve that is close to the measured shrinkage. The best fit line, the residual values (R), and the coefficient of error values (M) may be used to indicate the better accuracy of the modified models

3. Materials and Method

3.1. Mix Proportion

The repair materials used in this research were cement-based mortar reinforced with polymer-based monofilament micro synthetic fibers (see Figure 1). The properties of the fiber are shown in Table 1. It is an alkali resistant and non-corrosive material with a tensile strength of 900 MPa. The fiber type is a monofilament with the diameter of filament being 27 micron and its length, 12 mm. The amount of fiber incorporated into the mixtures (fiber dosage by weight of mortar) varied from 0% to 0.12%. The cement/sand ratio was controlled at 0.5 for all the mixtures. Meanwhile, the w/c ratio of the mixtures was set at 0.35. Furthermore, a chloride-free liquid admixture for set acceleration and rapid hardening of cement based-mortar, i.e., Sika accelerator, was used at 10% by weight of cement. This amount of the accelerator was selected on the basis of several trial mixes to obtain repair mortar with a minimum compressive strength of 15 MPa at 1 day of age. The accelerator partially substituted the water content of the mixtures to keep the total water-to-cement ratio at 0.35. Table 2 shows the composition of the micro-synthetic fiber-reinforced mortar mixtures.

3.2. Specimens Preparation and Shrinkage Test

Three cylinder specimens with a diameter of 75 mm and a height of 275 were cast for each mix. The slenderness of each specimen was within the range specified in the RILEM Recommendation [25]. On the following day after casting, the specimens were demolded and the specimens were wrapped with a dry cloth to remove any excess moisture on the surface of the specimens. Subsequently, four pairs of demec points were attached on the surface of the specimens at an equidistance of 90°. The gauge length of the demec points was 200 mm (see Figure 2). This length was assigned as an initial length (L) before shrinkage occurred.



Figure 1. Monofilament micro-synthetic fibers.

Table 1. Properties of micro-synthetic fiber [24].

Category	Properties
Fiber class	EN 14889-2 Class 1
Raw material	100% Polyamide 6.6
Fiber type	Monofilament
Specific gravity	1.14 gr/cm ³
Length	12 mm
Filament diameter	27 micron
Tensile strength	900 MPa
Elongation at break	17.55%
Melting point	260 °C
Alkali resistance	Excellent
Resistance to corrosion	Excellent
Number of fibers/kg	111,000,000

Table 2. Mix Proportion of micro-synthetic fibre-reinforced mortar.

Specimen ID	Fiber Dosage	Cement (kg/m ³)	Fine Aggregate (Sand) (kg/m ³)	Water (lt/m ³)	Accelerator (lt/m ³)	Micro-Synthetic Fiber (kg/m ³)
RMM 0%	0.00%	800	1600	200	80	0.00
RMM 0.04%	0.04%	800	1600	200	80	0.40
RMM 0.06%	0.06%	800	1600	200	80	0.60
RMM 0.08%	0.08%	800	1600	200	80	0.80
RMM 0.10%	0.10%	800	1600	200	80	1.00
RMM 0.12%	0.12%	800	1600	200	80	1.20

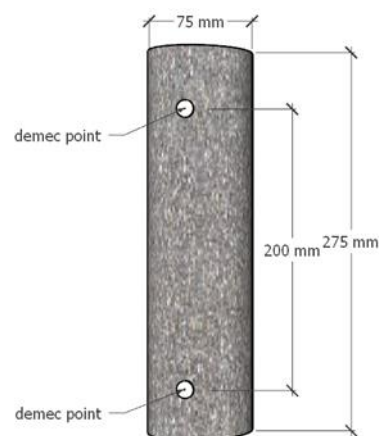


Figure 2. Shrinkage specimen.

Shrinkage of the specimens was determined by measuring the change in the distance between a pair of demec points using a demountable mechanical gauge (Demec Gauge) as shown in Figure 3. The specimens were stored in a laboratory room temperature (26° C) and humidity (85%) during the measurement period. The temperature and humidity represent a seasonal environment in some parts of Indonesian territory. Measurement of the change in length was started at 1 day of age and an average of four readings from four pairs of demec points was taken (ΔL) in each specimen. The measurement was carried out continuously until 84 days of age. The shrinkage of the specimens was calculated by the following equation:

$$\epsilon_{sh(t)} = \frac{\Delta L_t}{L} \tag{5}$$

where $\epsilon_{sh(t)}$ is the shrinkage at time t , ΔL_t is the average change in length after time t , and L is the original length (200 mm).

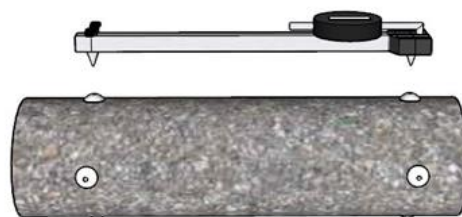


Figure 3. Measuring shrinkage with damage gauge.

4. Results and Discussion

4.1. Shrinkage Development with Time

The measured shrinkage of the micro-synthetic fiber-reinforced mortars is presented in Figure 4. The results indicate that a very rapid shrinkage development occurs at an early age. The 3-day shrinkage of the mortars is already in the range of 40–50% of the 84-day shrinkage. After 14 days of age, the development of shrinkage is almost negligible; the 14-day shrinkage of the mortars already attains about 95–98% of the 84-day shrinkage. The nearly horizontal trend of the shrinkage curves after 14 days also suggests that the difference between the 84-day shrinkage and the ultimate shrinkage value is trivial.

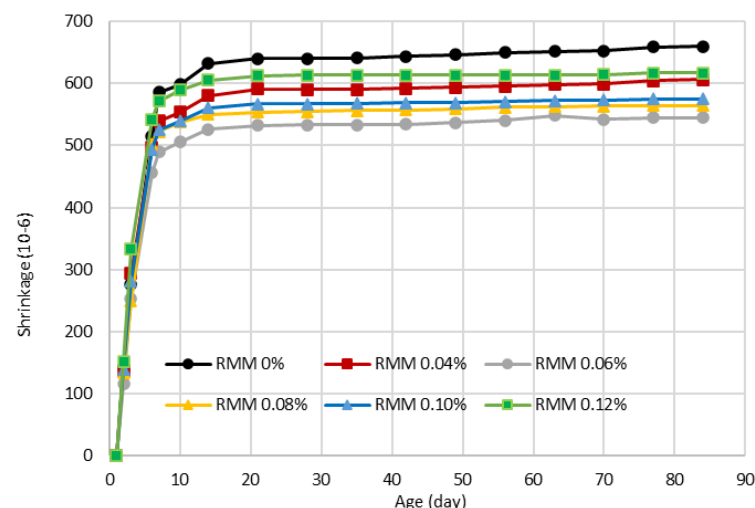


Figure 4. The shrinkage development with time.

The above shrinkage behavior is very dissimilar to normal concrete shrinkage. Generally, the shrinkage of concrete increases at a diminishing rate [26]. However, the development of normal concrete shrinkage at an early time is not as rapid as that of the micro-synthetic fiber-reinforced mortar. The ACI 209.2R-08 suggests that the shrinkage

half-time is achieved at 35 to 55 days depending on the curing time and type. This range of the shrinkage half-time is obviously longer than the observed shrinkage half-time of the micro-synthetic fiber-reinforced mortar. Apparently, half of the ultimate shrinkage value of the micro-synthetic fiber-reinforced mortar can be achieved at 3 days (see Figure 4). Nevertheless, the magnitude of the ultimate shrinkage of the micro-synthetic fiber-reinforced mortar is comparable with most of the ultimate shrinkage of concrete.

The rapid development of shrinkage at an early age of the micro-synthetic fiber-reinforced mortar could be related to the rapid strength development of this material due to the use of an accelerator. The influence of alkali-free liquid accelerator on the shrinkage of concrete has been investigated by Sheng et al. [18]. They noted that the rate of shrinkage is faster in concrete containing a higher dosage of the accelerator. At 9 wt% of accelerator, they found a rapid development of shrinkage at an early age. After 14 days, the shrinkage curve approached an asymptotic trend. This behavior is in line with the shrinkage behavior of the micro-synthetic fiber-reinforced mortar investigated in this study.

In the meantime, the influence of adding micro-synthetic fibers can also be observed from Figure 4. Generally, the fibers reduce the magnitude of the shrinkage but they do not affect the shrinkage rate. The influence of fiber can be explained via the following mechanism: once the mortar shrinks, shear stress is induced between the fiber and the surrounding mortar. This shear stress, in turn, influences the mortar deformation behavior, resulting in macroscopic composite shrinkage lower than that of a pure cement-based mortar [27]. The influence of fibers on the shrinkage depends on the fiber volume fraction. Based on the 84-day shrinkage value shown in Figure 5, a fiber dosage of 0.06% gives the greatest reduction of the shrinkage. This finding is in agreement with Bandelj et al. [28], who noted that with an increase in the fiber content, the shrinkage was reduced only up to a certain fiber content. An excess of fiber content would result in poor workability and shrinkage.

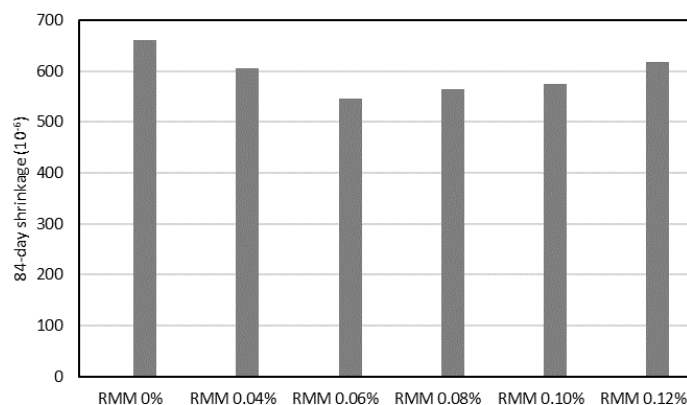


Figure 5. The influence of fiber volume fraction on the 84-day shrinkage.

4.2. Comparison with the Prediction Models

The shrinkage prediction models of ACI 209.2R-08 (Equation (1)) and CEB-MC 90-99 (Equation (2)) are applied in this study. Figure 6 shows examples of comparison between the measured shrinkage and the predicted shrinkage. As expected, there is a distinct trend of the shrinkage curve between the measured shrinkage and the predicted shrinkage. Both ACI 209.2R-08 and CEB-MC 90-99 models show a slower shrinkage rate at an early age than the measured shrinkage. This difference in the shrinkage behavior can be related to the use of an accelerator that causes the rapid development of shrinkage at an early age in the micro-synthetic fiber-reinforced mortar, as discussed in the preceding section.

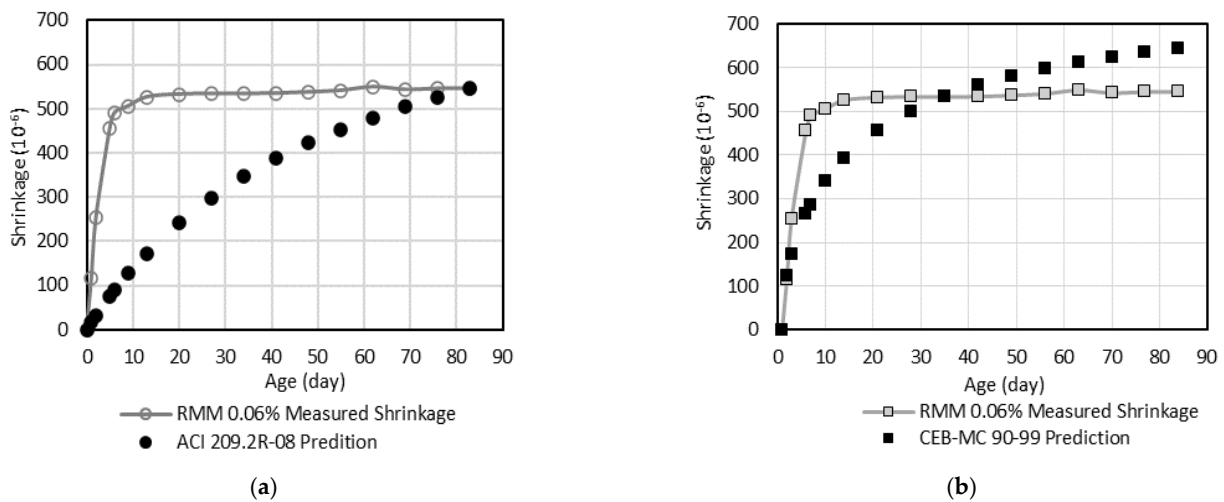


Figure 6. Comparison between the measured shrinkage and the predicted shrinkage by ACI 209.2R-08 (a) and CEB-MC 90-99 (b) models.

The differences in the prediction may be quantitatively evaluated using the method of best fit line, residual values (R), or the coefficient of error values (M). Figure 7 shows the relationship between the measured shrinkage and the predicted shrinkage. The relationship is assessed by a linear regression analysis to determine the best fit line and the results are indicated in the figure. Meanwhile, the difference values between the measured shrinkage and the predicted shrinkage (residual values) have been plotted in Figure 8. Both Figures 7 and 8 clearly indicate that the predicted shrinkage, significantly, is lower than the measured shrinkage, especially at an early age. However, the residual values of the shrinkage estimated using CEB-MC 90-99 are positive at a later age (see Figure 8b). The positive values correspond to a higher predicted shrinkage value after 40 days of age, as shown in Figure 6b. Finally, the prediction models are assessed by the coefficient of error method using Equation (4). Table 3 summarizes the results of the quantitative evaluations of the prediction models. In general, it is concluded that the shrinkage prediction models do not accurately estimate the shrinkage behavior of the micro-synthetic fiber-reinforced mortar. Therefore, improvement of the models is needed, as discussed in the following section.

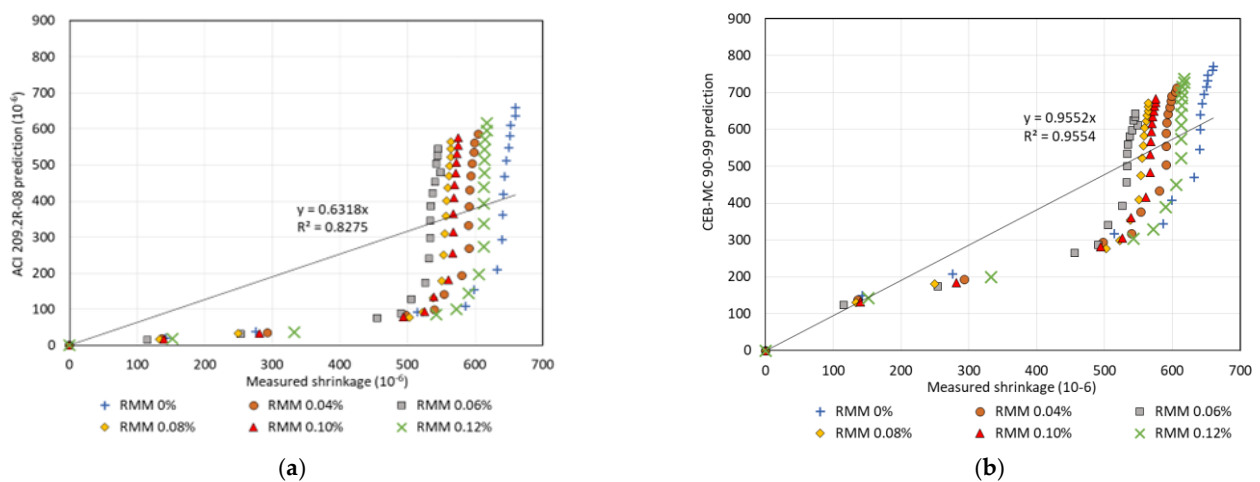


Figure 7. Evaluation of the ACI 209.2R-08 (a) and CEB-MC 90-99 (b) models by best fit line method.

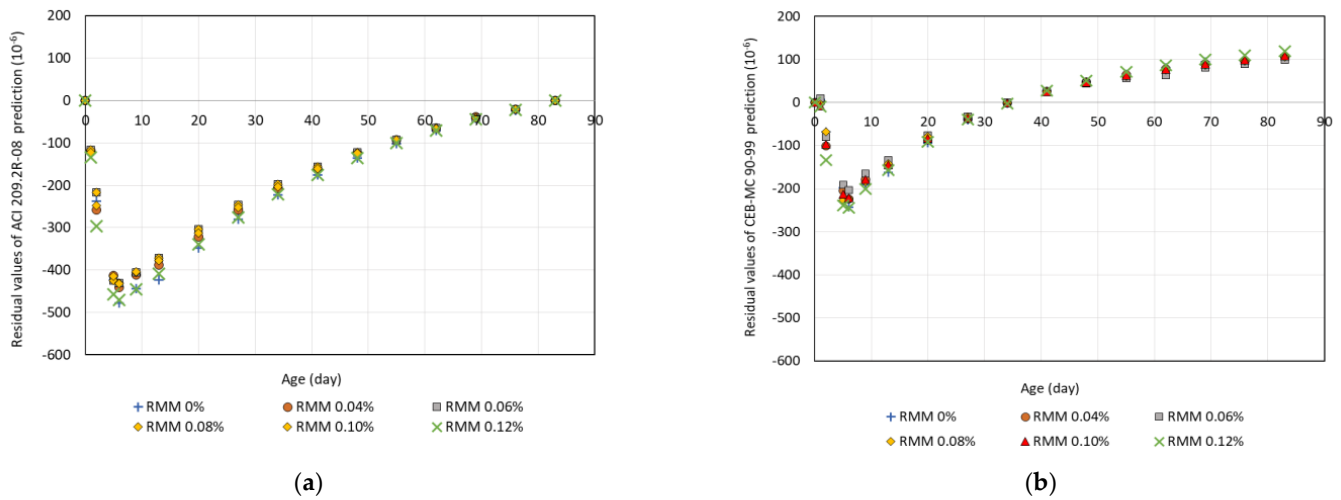


Figure 8. Evaluation of the ACI 209.2R-08 (a) and CEB-MC 90-99 (b) models by residual analysis.

Table 3. Summary of quantitative evaluation of shrinkage prediction models.

Method	ACI 209.2R-08	CEB MC 90-99
Best fit line	$y = 0.6318 x$ $R^2 = 0.8275$	$y = 0.9552 x$ $R^2 = 0.9554$
Residual values (R)	−207.73	−26.51
Coefficient of error (M)	161.83%	73.97%

4.3. Improvement of the Models

It has been shown in Section 4.1 that the shrinkage curve of the micro-synthetic fiber-reinforced mortar shows the rapid development of shrinkage at an early age. At 3 days of age, the magnitude of shrinkage already attains about 40–50% of the 84-day shrinkage. It is also indicated that the curve is approaching an asymptotic value after 14 days. Considering the above trend, both ACI 209.2R-08 and CEB-MC 90-99 models should be modified to reflect this trend. In the ACI 209.2R-08 model, the time ratio of Equation (1) determines the development of shrinkage with time. The value of f in the time ratio signifies the rate of shrinkage. Its value represents the shrinkage half-time. Hence, to depict the rapid development of shrinkage at an early time, the value of f in the ACI 209.2R-08 model can be modified to reflect the shrinkage half-time of the micro-synthetic fiber-reinforced mortar. In this study, firstly we modify the f value to be 3 days. The resulting modified ACI 209.2R-08 is then used to predict the shrinkage behavior of the micro-synthetic fiber-reinforced mortar. The predicted shrinkage is assessed using the coefficient of error method. If the value of the coefficient of error is not satisfied (greater than 30%), we try another f value either lower or higher than 3 days until a minimum coefficient of error is obtained. In this way, we propose f is equal to 2 days and, so, Equation (1) can be written as follows:

$$\epsilon_{sh(t,t_c)} = \left(\frac{t - t_c}{2 + t_c} \right) \times \epsilon_{sh(u)} \tag{6}$$

A similar procedure is employed to modify the CEB-MC 90-99 model. In the model, the shrinkage development with time is represented by Equation (3). In the equation, a value of 350 signifies the shrinkage rate. Thus, this value should be modified to reflect the rapid shrinkage development of the micro-synthetic fiber-reinforced mortar at an early age. Based on several trials, we propose to modify the 350 value to 50, since this value gives

the lowest coefficient of error. So, Equation (3) of the CEB-MC 90-99 model is modified as follows:

$$\beta_s(t - t_c) = \left[\frac{(t - t_c)/t_1}{50[(V/S)/(V/S_0)]^2 + (t - t_c)/t_1} \right]^{0.5} \tag{7}$$

Figure 9 shows examples of the comparison between the curves of the measured shrinkage and the predicted shrinkage using the modified ACI 209.2R-08 and the modified CEB-MC 90-99 models. The figure indicates that the shrinkage behavior of the micro-synthetic fiber-reinforced mortar can now be estimated quite accurately using the modified models. Figures 10 and 11 demonstrate the improved correlation between the measured shrinkage and predicted shrinkage when it is assessed using the best fit line and residual analysis method, respectively. Meanwhile, Table 4 summarizes the quantitative improvements of the modified models compared to the originals.

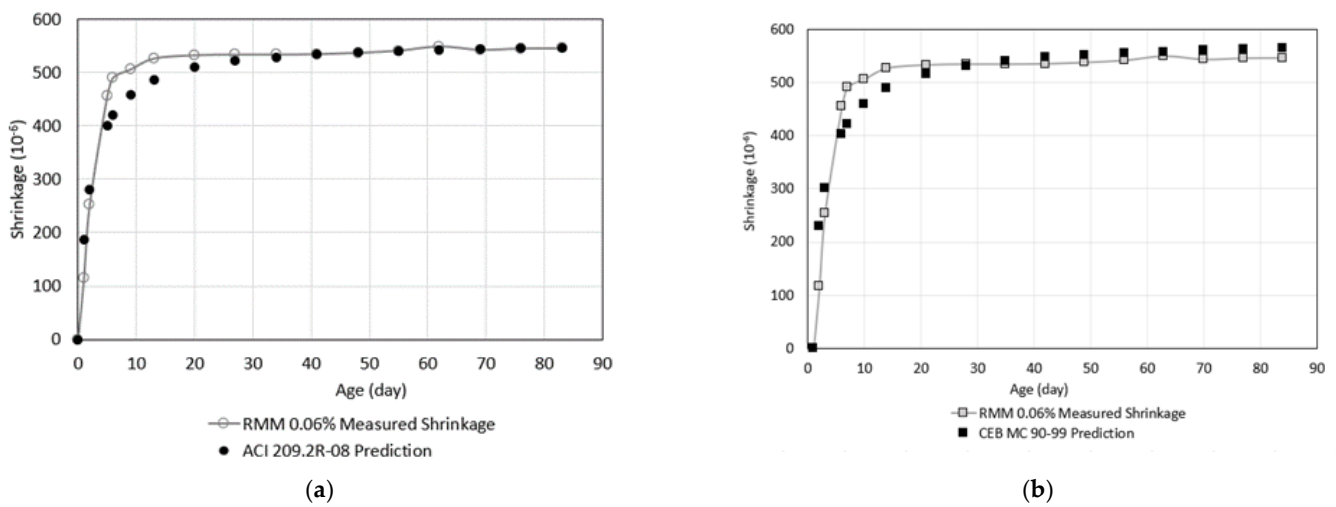


Figure 9. Comparison between the measured shrinkage and the predicted shrinkage by the modified ACI 209.2R-08 (a) and the modified CEB-MC 90-99 (b) models.

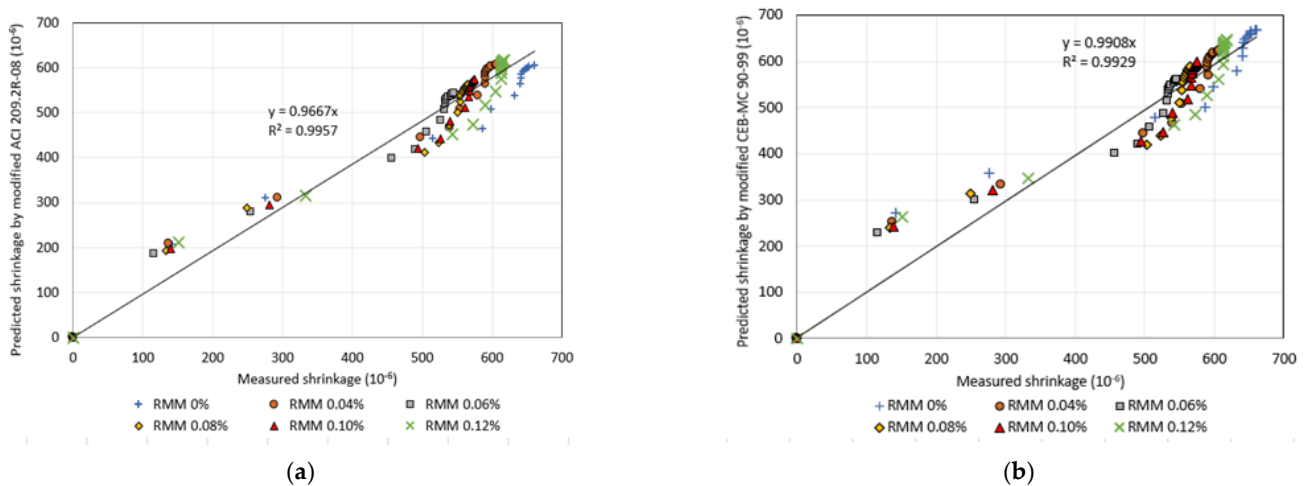


Figure 10. Evaluation of the modified ACI 209.2R-08 (a) and the modified CEB-MC 90-99 (b) models by best fit line method.

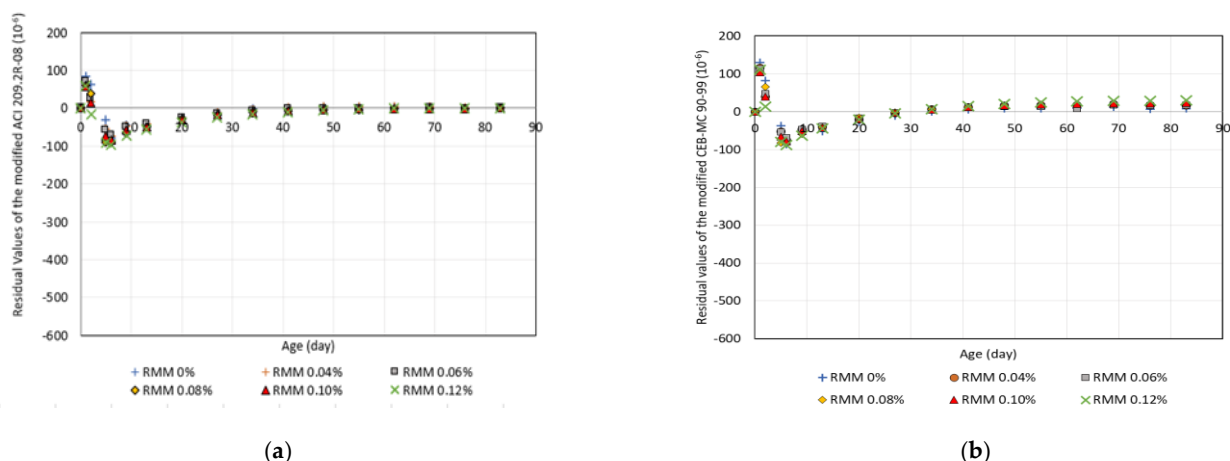


Figure 11. Evaluation of the modified ACI 209.2R-08 (a) and the modified CEB-MC 90-99 (b) models by residual analysis.

Table 4. Summary of quantitative evaluation of the modified and original prediction models.

Method	ACI 209.2R-08	CEB-MC 90-99	Modified ACI 209.2R-08	Modified CEB-MC 90-99
Best fit line	$y = 0.6318 x$ $R^2 = 0.8275$	$y = 0.9552 x$ $R^2 = 0.9554$	$y = 0.9667 x$ $R^2 = 0.9957$	$y = 0.9908 x$ $R^2 = 0.9929$
Residual values (R)	-207.73	-26.51	-14.14	1.28
Coefficient of error (M)	161.83%	73.97%	20.53%	26.74%

5. Conclusions

This study leads to the following conclusions:

- The shrinkage behavior of the micro-synthetic fiber-reinforced mortar shows rapid development of shrinkage at an early age. The inclusion of fibers does not influence the shrinkage rate, but does affect the magnitude of shrinkage. The lowest shrinkage occurs in the mixture with a fiber dosage of 0.06%.
- The shrinkage rapid development of the micro-synthetic fiber-reinforced mortar at an early age is characterized by a shorter shrinkage half-time (3 days) and a faster trend of reaching asymptotic value (after 14 days) than shrinkage of normal concrete.
- The shape of the shrinkage curve of the micro-synthetic fiber-reinforced mortar cannot be accurately estimated by the ACI 209.2R-08 and CEB-MC 90-99 models. The difference between the measured shrinkage and the predicted shrinkage by these models has been evaluated quantitatively using the method of best fit line, residual analysis, and coefficient of error. The quantitative evaluations indicate a high erroneousness.
- The ACI 209.2R-08 and CEB-MC 90-99 models have been modified in such a way to reflect the shrinkage behavior of the micro-synthetic fiber-reinforced mortar. The modified models give fairly accurate prediction of the shrinkage.

Author Contributions: Conceptualization, S.A.K.; methodology, S.A.K. and E.S.; formal analysis, R.A.K. and S.A.K.; investigation, R.A.K. and E.S.; writing—original draft preparation, R.A.K.; writing—review and editing, S.A.K. and E.S.; visualization, R.A.K. and S.A.K.; funding acquisition, S.A.K. All authors have read and agreed to the published version of the manuscript.

Funding: This research was funded by SEBELAS MARET UNIVERSITY, contract number 2550/UN27.22/PT.01.03/2022.

Institutional Review Board Statement: Not applicable.

Informed Consent Statement: Not applicable.

Data Availability Statement: Not applicable.

Acknowledgments: Authors would like to sincerely thank Kratos for providing the micro-synthetic fibers used in this research.

Conflicts of Interest: The authors declare no conflict of interest.

References

1. Haddad, R.H.; Shannag, M.J.; Al-Hambouth, M.T. Repair of reinforced concrete beams damaged by alkali-silica reaction. *ACI Struct. J.* **2008**, *105*, 145–153. [\[CrossRef\]](#)
2. Bhikshma, V.; Reddy, M.K.; Sunitha, K. Experimental study on rehabilitation of RC beams using epoxy resins. *Asian J. Civ. Eng.* **2010**, *11*, 533–542.
3. Park, S.K.; Yang, D.S. Flexural behavior of reinforced concrete beams with cementitious repair materials. *Mater. Struct. Constr.* **2005**, *38*, 329–334. [\[CrossRef\]](#)
4. Jumaat, M.; Kabir, M.H.; Obaydullah, M. A Review of the Repair of Reinforced Concrete Beams. *J. Appl. Sci. Res.* **2006**, *2*, 317–326.
5. Jumaat, M.Z.B.; Kabir, M.H.; Obaydullah, M. Structural performance of reinforced concrete beams repairing from spalling. *Eur. J. Sci. Res.* **2010**, *45*, 89–102.
6. Kristiawan, S.A.; Saifullah, H.A.; Supriyadi, A. Influence of Patching on the Shear Failure of Reinforced Concrete Beam without Stirrup. *Infrastructures* **2021**, *6*, 97. [\[CrossRef\]](#)
7. Turcry, P.; Loukili, A.; Haidar, K.; Pijaudier-Cabot, G.; Belarbi, A. Cracking Tendency of Self-Compacting Concrete Subjected to Restrained Shrinkage: Experimental Study and Modeling. *J. Mater. Civ. Eng.* **2006**, *18*, 46–54. [\[CrossRef\]](#)
8. Baluch, M.H.; Rahman, M.K.; Al-Gadhib, A.H. Risks of Cracking and Delamination in Patch Repair. *J. Mater. Civ. Eng.* **2002**, *14*, 294–302. [\[CrossRef\]](#)
9. Bhutta, A.; Farooq, M.; Banthia, N. Performance characteristics of micro fiber-reinforced geopolymer mortars for repair. *Constr. Build. Mater.* **2019**, *215*, 605–612. [\[CrossRef\]](#)
10. Tayeh, B.A.; Akeed, M.H.; Qaidi, S.; Bakar, B.H.A. Case Studies in Construction Materials Influence of microsilica and polypropylene fibers on the fresh and mechanical properties of ultra-high performance geopolymer concrete (UHP-GPC). *Case Stud. Constr. Mater.* **2022**, *17*, e01367. [\[CrossRef\]](#)
11. Sharma, S.K.; Kumar, A.A.; Ransinchung, G.D.R.N.; Kumar, P. Micro fiber reinforced cement paste and mortar overlays—A review. *Int. J. Pavement Res. Technol.* **2013**, *6*, 765–772. [\[CrossRef\]](#)
12. Banthia, N.; Azzabi, M.; Pigeon, M. Restrained shrinkage cracking in fibre-reinforced cementitious composites. *Mater. Struct.* **1993**, *26*, 405–413. [\[CrossRef\]](#)
13. Aly, T.; Sanjayan, J.G. Shrinkage-cracking behavior of OPC-fiber concrete at early-age. *Mater. Struct. Constr.* **2010**, *43*, 755–764. [\[CrossRef\]](#)
14. Bissonnette, B.; Pierre, P.; Pigeon, M. Influence of key parameters on drying shrinkage of cementitious materials. *Cem. Concr. Res.* **1999**, *29*, 1655–1662. [\[CrossRef\]](#)
15. Al-musawi, H.; Figueiredo, F.P.; Guadagnini, M.; Pilakoutas, K. Shrinkage properties of plain and recycled steel—Fibre-reinforced rapid hardening mortars for repairs. *Constr. Build. Mater.* **2019**, *197*, 369–384. [\[CrossRef\]](#)
16. Kristiawan, S.A. Evaluation of Models for Estimating Shrinkage Stress in Patch Repair System. *Int. J. Concr. Struct. Mater.* **2012**, *6*, 221–230. [\[CrossRef\]](#)
17. Bouziadi, F.; Boulekbache, B.; Hamrat, M. The effects of fibres on the shrinkage of high-strength concrete under various curing temperatures. *Constr. Build. Mater.* **2016**, *114*, 40–48. [\[CrossRef\]](#)
18. Sheng, Y.; Xue, B.; Li, H.; Qiao, Y.; Chen, H.; Fang, J.; Xu, A. Preparation and Performance of a New-Type Alkali-Free Liquid Accelerator for Shotcrete. *Adv. Mater. Sci. Eng.* **2017**, *2017*. [\[CrossRef\]](#)
19. *ACI Committee 209*; *ACI 209.2R-08 Guide for Modeling and Calculating Shrinkage and Creep in Hardened Concrete*. ACI: Farmington Hills, MI, USA, 2008.
20. Comite Euro-International du Beton. *CEB-FIP Model Code 1990*; Thomas Telford Ltd.: London, UK, 1990; pp. 57–58.
21. Kristiawan, S.; Sangadji, S. Prediction model for shrinkage of lightweight. *Asian J. Civ. Eng.* **2009**, *10*, 1–11.
22. Kristiawan, S.A.; Aditya, M.T.M. Effect of high volume fly ash on shrinkage of self-compacting concrete. *Procedia Eng.* **2015**, *125*, 705–712. [\[CrossRef\]](#)
23. Pasalli, D.A.; Tudjono, S.; Nurhuda, I. A Creep Prediction Model for Concrete Made from Pit Sand with Low Silica Content. *Infrastructures* **2022**, *7*, 134. [\[CrossRef\]](#)
24. Kratos Fibers. Available online: https://kratosreinforcement.com/wp-content/uploads/2022/05/KratosBrosur_ENDONEZYA_DUSUK_043.pdf (accessed on 17 December 2022).
25. RILEM Technical Committees 129. RILEM TC 129-MHT Part 9: Shrinkage for service and accident conditions. *Mater. Struct. Constr.* **2000**, *33*, 224–228.
26. Wang, Y.; Zhu, J.; Guo, Y.; Wang, C. Early shrinkage experiment of concrete and the development law of its temperature and humidity field in natural environment. *J. Build. Eng.* **2023**, *63*, 105528. [\[CrossRef\]](#)

27. Zhang, J.; Li, V.C. Influences of Fibers on Drying Shrinkage of Fiber-Reinforced Cementitious Composite. *J. Eng. Mech.* **2001**, *127*, 37–44. [[CrossRef](#)]
28. Bandelj, B.; Saje, D.; Šušteršič, J.; Lopatič, J.; Saje, F. Free Shrinkage of High Performance Steel Fiber Reinforced Concrete Free Shrinkage of High Performance Steel Fibre Reinforced Concrete. *J. Test. Eval.* **2011**, *39*, 166–176. [[CrossRef](#)]

Disclaimer/Publisher’s Note: The statements, opinions and data contained in all publications are solely those of the individual author(s) and contributor(s) and not of MDPI and/or the editor(s). MDPI and/or the editor(s) disclaim responsibility for any injury to people or property resulting from any ideas, methods, instructions or products referred to in the content.